



Preparation of Cerium-Hierarchical SAPO-34 Catalyst and Presentation of a Kinetic Model for Methanol to Propylene Process (MTP)

Masoumeh Ghalbi-Ahangari^{1*}, Ali Taheri-Najafabadi², Parviz Rashidi-Ranjbar², Zahra Taheri¹

¹Research Laboratory, Research Institute of Petroleum Industry (RIPI), Tehran, Iran

²Faculty of Chemistry, Department of Chemistry, University of Tehran, Tehran, Iran

(Received 15 Aug. 2019; Final revised received 15 Jan. 2020)

Abstract

In this paper, a new lumped kinetic model for methanol to propylene process (MTP) over Cerium-Hierarchical SAPO-34 catalyst was developed based on data obtained from a micro catalytic reactor in the temperature range of 390–450°C and at atmospheric pressure, using appropriate reaction network. The Ce-HSAPO-34 zeolite was synthesized by hydrothermal method in the presence of n-propylamine as a mesoscale template and pore size modifier. The reaction rate equation has been introduced with consideration of reaction mechanism and the parameters were optimized on the experimental data by genetic algorithm. Comparing the experimental and predicted data showed that the predicted values from the presented model are well fitted to the experimental data.

Keywords: Kinetic modeling, methanol to propylene process, Lumped kinetic model, SAPO-34.

*Corresponding author: Masoumeh Ghalbi-Ahangari, Research Laboratory, Research Institute of Petroleum Industry (RIPI), P.O. Box 14665-1998, Tehran, Iran. E-mail: ahangarym@ripi.ir.

Introduction

Propylene, with chemical formula of $\text{CH}_3\text{CH}=\text{CH}_2$, undoubtedly is one of the oldest and earliest raw materials for the production of polypropylene, acrylonitrile, propylene oxide, Oxo alcohols and Cumene in the petrochemical industry. Due to the increasing demand for propylene and rapid depletion of oil resources, new processes with high propylene yield are needed[1-3]. The methanol to propylene (MTP) process is regarded as a promising alternative route for the high yield production of propylene. The modified SAPO-34 catalyst shows an exceptional selectivity for propylene and the complete conversion of methanol in the MTP reaction, although it is rapidly deactivated by coke[4]. In recent decades, one of the successful processes for reducing diffusion limitations of SAPO-34 is the extension of hierarchical SAPO-34, which is referred as a bimodal pore system (mesoporous and microporous). On the other hand, mesoporous structure in hierarchical SAPO-34 provides an ideal location as active phases, for deposition metals and metal oxides. The incorporation of metal particles into SAPO-34 framework results in development of crystalline materials with different textural properties and deep alterations of acidic and catalytic performance of SAPO-34[5].

Kinetic models are essential for reactor design, modeling and optimization of processes. They are implemented in mathematical models of various reactors for estimation of product selectivity, product distribution and determination of the dimensions of the reactor [6]. Few researchers focused on MTO/MTP reaction pathway and its related kinetic model. Due to the complexity of the reaction network of the methanol conversion into light olefins, most of the kinetic studies in MTO/MTP processes are lumped models which are commonly developed based on "Hydrocarbon pool" mechanism [7-9]. Methanol formed dimethyl ether, which was converted to hydrocarbon pool. The carbon pool is continuously building up and breaking up to yield methane, ethylene, propylene, butene, pentene and coke.

In the present study, hierarchical SAPO-34 is synthesized, by using of n-propylamine (NPA) and Cerium nitrate to enhance the catalyst selectivity to propylene. The kinetic model for the MTP process is studied on modified SAPO-34 catalyst in a fixed bed reactor, based on the simple and reliable reaction network. The modified mechanism of methanol to olefin as proposed by Ali Taheri Najafabadi et al. [10] has been utilized for common SAPO-34 catalysts and the effect of Cerium-Hierarchical SAPO-34 on reaction pathways and reaction rate parameters has been studied. The reaction rate equation has been introduced with consideration of reaction mechanism and the parameters were optimized on the experimental data by genetic algorithm. Consequently, a heterogeneous model in which the reaction was assumed to occur in the solid catalytic bed was obtained.

Experimental

Materials

Tetraethyl ammonium hydroxide (TEAOH, 20wt.% aqueous solution), methanol (MeOH, 99.9%) and ortho-phosphoric acid (H₃PO₄, 85 wt%), were purchased from Merck. Aluminum isopropoxide (AIP, 97 wt.%), fumed silica (FS, 98 wt.%) and n-propylamine (NPA, 99 wt.%), purchased from Aldrich. All chemical reagents were of analytical grade and used as received without further purification.

Catalyst preparation

The catalyst was prepared according to the hydrothermal method described in our previous works [11]. To prepare HSAPO-34, a certain amount of aluminum isopropoxide (98%, Merck) dissolved in deionized water and ortho-phosphoric acid (H₃PO₄, 85 wt%) was added to the solution drop wise while stirring the reaction mixture for additional 30 minutes; then fumed silica was added to the solution and stirred vigorously until a homogeneous solution formed.

Then, definite amounts of tetraethyl ammonium hydroxide (TEAOH, 20 % aqueous solution) and n-propylamine (NPA) were added drop wise to the mixture. The resultant gel was allowed to age and hydrolyze at room temperature for 24 h. Finally, the precursor gels were transferred into Teflon-lined stainless steel autoclaves for hydrothermal treatment at 200 °C for 12 h under autogenously pressure. The solid products were recovered and washed four times by centrifugation, dried at 120 °C and calcined at 550 °C in air flow for 6h to remove the organic components.

Ce-HSAPO-34 catalyst was prepared using sequential impregnation by cerium nitrate to achieve a Hierarchical SAPO-34 having 0.5 % cerium oxide. For this purpose, certain amount of cerium nitrate hexahydrate was dissolved in deionized water and added to the suspension of HSAPO-34 while stirring. The resulting product was dried at 120 °C and calcined at 550 °C for 6h.

Packed bed reactor

The experimental data was carried out in a fixed bed down flow Pyrex reactor (50 cm high and 1.1cm internal diameter) at atmospheric pressure. 1g of synthesis catalyst (20–40 mesh) was loaded into the reactor in each run. The heat transfer to the reactor was provided by an electric jacket wrapped around the reactor. Reaction temperature was controlled by a PID controller and measured by a thermocouple located at the center of the catalyst bed. To increase the olefin's selectivity and reduce the rate of catalyst's deactivation, the feed was enriched with water vapor. Water-methanol mixture was fed together with N₂ as diluent at a flow rate of 60 mL/min. The experiments were performed in a temperature range from 390 to 450 °C using weight hour space velocity (WHSV) of

1.03, 2.03 and 3.75 grMeOH.grCatalyst⁻¹.hr⁻¹. In all experimental runs, when steady state conditions were established a portion of the gas mixture leaving the reactor was analyzed using an on-line gas chromatograph (Agilent 6890 GC, PONA and Al₂O₃ capillary columns, TCD and FID detectors). Such a procedure was repeated at regular time intervals of 5 min.

Results and discussion

Catalyst characterization

X-ray diffraction pattern of the catalyst was taken in order to characterize the phases and crystallinities of the Ce-H-SAPO-34 zeolite. The synthesized catalyst was analyzed at room temperature by X-ray diffraction using PHILIPS- PW1840 diffractometer with Cu/K α radiation ($\lambda=1.5406$ Å). The samples were analyzed at a scanning rate of 3°/min, from 1° to 50° (an angular range 2θ). The XRD pattern of the catalyst is shown in Figure 1. It indicates the presence of the SAPO-34 characteristic peaks and the existence of Cerium oxide species does not disrupt strongly the crystalline framework of hierarchical SAPO-34[12].

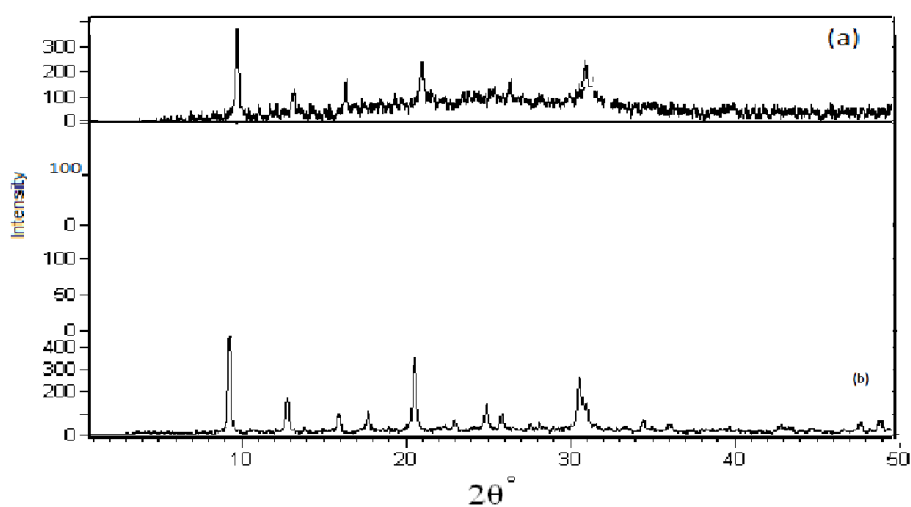


Figure 1. Powder XRD patterns of (a) conventional SAPO-34, (b) Ce-H-SAPO-34.

The surface morphology and crystallite size of Ce-H-SAPO-34 was determined by field emission scanning electron microscopy (Philips XL30 scanning electron microscope), is shown in Figure 2. The SEM images of Ce-H1-SAPO-34 sample show the characteristic cubic morphology of the CHA crystals with particle size of 1.1 μm [13].

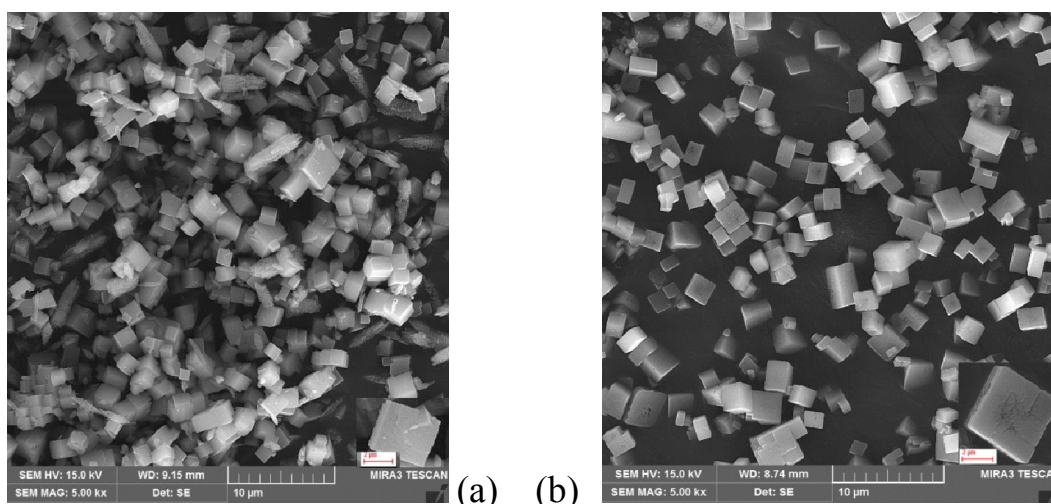


Figure 2. FE-SEM images of (a) conventional SAPO-34 and (b) Ce-H-SAPO-34.

The acidity and strength of acid sites of the catalysts were characterized by NH_3 -TPD technique (Micrometrics TPD/TPR 2900) and presented in Table 1. The desorption temperature signifies the strength of acid sites and the area under each corresponding peak indicates the amount of NH_3 desorbed, which is proportional to acidity. The Ce-H1-SAPO-34 showed two desorption peaks around 200°C and 400°C . The first peak attributed to the weak acidic sites and the second peak attributed to the strong acidic sites. In the Ce-H-SAPO-34, the amounts of both weak and strong acidic sites have decreased compared to the unmodified hierarchical SAPO-34[14].

Table 1. NH_3 -TPD data and the acidic amount of SAPO-34, H1-SAPO-34 and Ce-H1-SAPO-34.

Sample	Acid amount (mmol/g)		Peak temperature ($^\circ\text{C}$)	
	Weak acidity	Strong acidity	TP1 ^a	TP2 ^b
SAPO-34	1.48	1.77	198	398
Ce-H1-SAPO-34	0.95	0.99	174	380

Kinetic study

A lumped kinetic model was proposed based on the reaction network presented by A. Taheri Najafabadi et al [10]. That kinetic modeling performed based on data obtained on the common microporous SAPO-34 catalysis. The Hierarchical SAPO-34 in present work has a bimodal pore structure (mesoporous and microporous) with lower acidity compared to common micro porous SAPO-34 catalyst. Changing the catalyst structure and its surface properties might change the reaction path and product distribution. A new 12 reaction networks for Hierarchical SAPO-34 are presented in Table 2. The first step in the overall sequence of the conversion of methanol to hydrocarbons is the conversion of methanol to DME (Experimental studies show that DME is

formed in the initial stages of the reaction prior to the production of any hydrocarbon products). DME and methanol rapidly reach equilibrium over the catalyst surface, and so either can contribute as a feedstock to produce hydrocarbon products. Ethylene is primary product formed from methanol and DME. Based on the most accepted mechanism, the reactants methanol and DME as the methylation agents are repeatedly added to the organic reaction centers for the assembly of light olefins [15-19]. Therefore, the reactions 3-6 have been introduced. These organic species act as catalytic hosts (co-catalyst) in MTO reaction. For SAPO-34 catalyst with strong acidity, the main portion of methanol would convert to ethylene and no more methanol present in hydrocarbon pool to react successively with lower olefins [18-19]. Commonly, the DME is considered as a dominant species for methylation agents in hydrocarbon pool [19]. For Hierarchical SAPO-34 with moderate acidity and lower cracking capability, both methanol and DME may participate in hydrocarbon pool to make higher molecular weights olefins. Based on reaction scheme introduced in Table 2, a 12 elementary reaction rate expression, that is summarized in Table 3, has been assumed and all 24 kinetic parameters has been found from experimental data. The equilibrium constant (K) of Reaction (R-1) calculated from experimental relationship found by Gayubo et al. [15] over ZSM-5 catalyst as follows:

$$-R\ln K_p = \frac{\Delta G}{T} = -\frac{4163}{T} + 2 \ln T - 1.01 \times 10^{-3}T - 5.82 \times 10^{-6}T^2 - 10.76 \quad 1$$

All other reaction is elementary and the order of reactions (R-2) and (R-3) in the reaction rate expression assumed to be 1, as observed by Bos et al.[16].

Table 2.The new 12 reaction network for MTP process.

$2\text{MeOH} \xrightleftharpoons{K_{r1}} [(\text{CH}_3)_2\text{O}] + \text{H}_2\text{O}$	(1)
$2[(\text{CH}_3)_2\text{O}] \xrightarrow{k_{r2}} \text{C}_2\text{H}_4 + 2 \text{MeOH}$	(2)
$2\text{MeOH} \xrightarrow{k_{r3}} \text{C}_2\text{H}_4 + 2\text{H}_2\text{O}$	(3)
$\text{C}_2\text{H}_4 + \text{DME} \xrightarrow{k_{r4}} \text{C}_3\text{H}_6 + \text{MeOH}$	(4)
$\text{C}_2\text{H}_4 + \text{MeOH} \xrightarrow{k_{r5}} \text{C}_3\text{H}_6 + \text{H}_2\text{O}$	(5)
$\text{C}_3\text{H}_6 + \text{DME} \xrightarrow{k_{r6}} \text{C}_4\text{H}_8 + \text{MeOH}$	(6)
$\text{C}_3\text{H}_6 + \text{MeOH} \xrightarrow{k_{r7}} \text{C}_4\text{H}_8 + \text{H}_2\text{O}$	(7)
$\text{C}_4\text{H}_8 + \text{DME} \xrightarrow{k_{r8}} \text{C}_5\text{H}_{10} + \text{MeOH}$	(8)
$\text{MeOH} \xrightarrow{k_{r9}} \text{CO} + 2\text{H}_2$	(9)
$\text{CO} + \text{H}_2\text{O} \xrightarrow{k_{r10}} \text{CO}_2 + \text{H}_2$	(10)
$\text{MeOH} + \text{H}_2 \xrightarrow{k_{r11}} \text{CH}_4 + \text{H}_2\text{O}$	(11)
$\text{C}_2\text{H}_4 + \text{H}_2 \xrightarrow{k_{r12}} \text{C}_2\text{H}_6$	(12)

Table 3. Reaction rate equation for MTP process.

$r_1 = k_{01} \cdot \exp\left(-\frac{E_1}{RT}\right) \cdot C_{MeOH}^2 - \frac{k_{01}}{K} \cdot \exp\left(-\frac{E_1}{RT}\right) \cdot C_{DME} \cdot C_{H_2O}$	(1)
$r_2 = k_{02} \cdot \exp\left(-\frac{E_2}{RT}\right) \cdot C_{DME}$	(2)
$r_3 = k_{03} \cdot \exp\left(-\frac{E_3}{RT}\right) \cdot C_{MeOH}$	(3)
$r_4 = k_{04} \cdot \exp\left(-\frac{E_4}{RT}\right) \cdot C_{DME} \cdot C_{C_2H_4}$	(4)
$r_5 = k_{05} \cdot \exp\left(-\frac{E_5}{RT}\right) \cdot C_{MeOH} \cdot C_{C_2H_4}$	(5)
$r_6 = k_{06} \cdot \exp\left(-\frac{E_6}{RT}\right) \cdot C_{DME} \cdot C_{C_3H_6}$	(6)
$r_7 = k_{07} \cdot \exp\left(-\frac{E_7}{RT}\right) \cdot C_{MeOH} \cdot C_{C_3H_6}$	(7)
$r_8 = k_{08} \cdot \exp\left(-\frac{E_8}{RT}\right) \cdot C_{DME} \cdot C_{C_4H_8}$	(8)
$r_9 = k_{09} \cdot \exp\left(-\frac{E_9}{RT}\right) \cdot C_{MeOH}$	(9)
$r_{10} = k_{10} \cdot \exp\left(-\frac{E_{10}}{RT}\right) \cdot C_{CO} \cdot C_{H_2O}$	(10)
$r_{11} = k_{11} \cdot \exp\left(-\frac{E_{11}}{RT}\right) \cdot C_{MeOH} \cdot C_{H_2}$	(11)
$r_{12} = k_{012} \cdot \exp\left(-\frac{E_{12}}{RT}\right) \cdot C_{C_2H_4} \cdot C_{H_2}$	(12)

Experimental data on Ce-H-SAPO-34

The experiments were carried out in a fixed bed reactor at three temperatures, i.e. 390°C, 420°C and 450°C and in three methanol space-time, i.e. 1.03, 2.03 and 3.57 (g of catalyst. h/mol of methanol fed). These data have been provided using 70 mol% water in the feed, in order to minimize the catalyst deactivation and total pressure inside the reactor was kept constant at 1.0 bar.

Modeling of the reactor

The model of the reactor was obtained by mass conservation equations on each chemical species (y_i). The predicted responses (y_i) are calculated from the following continuity equations, assuming plug flow in the experimental reactor:

$$\frac{d(y_i)}{d(W/F_{MeOH}^0)} = 100 \frac{M_i}{M_{MeOH}} \cdot R_i \quad i = 1, 2, \dots, m \quad 2$$

In this equation:

y_i	the yield of component i in g-formed per 100 g of methanol fed to the reactor
F_{MeOH}^0	the initial flow rate of methanol at the inlet of the reactor in moles/h
W	the amount of catalyst in g
W/F_{MeOH}^0	the space-time in g cat h/moles of methanol fed
M_i, M_{MeOH}	the molecular weight of species i and methanol

These differential equations can be solved using Gear's method numerically and with the initial condition of zero yields at zero space-time. The reactor products is compared with experimental data and the error function is calculated based on the function proposed by Froment[17-18]:

$$OF = \sum_{j=1}^m \sum_{l=1}^m w_{jl} \sum_{i=1}^n (y_{ij} - \widehat{y}_{ij}) \cdot (y_{il} - \widehat{y}_{il}) \quad 3$$

where (m) is the number of responses, (n) is the number of experiments, and (w_{jl}) is the elements of the inverse of the covariance matrix of the experimental errors on the responses (y).

Abraha et al. [19] have provided values for (w_{jl}) based on their statistical analyzes, they can be used as weight function. In this study, decimal genetic algorithm was used to estimate the parameters of the rate equations. Schematic of this algorithm is shown in Figure 3. A complete description of genetic algorithm techniques for parameter estimation has been provided by [20–22].

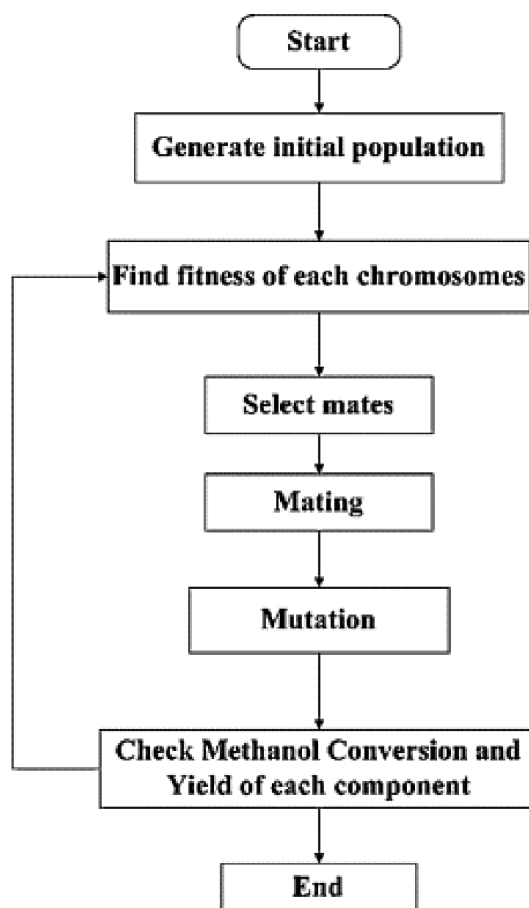


Figure 3. Flowchart of the genetic algorithm.

The initial guesses for activation energy are obtained by Evans–Polanyi equation [23]. Evans–Polanyi equation is related activation energy to energy released in the reaction and is presented as follows:

$$E_a = E_a^o - \alpha |\Delta H_r| \text{ for exothermic reaction} \quad 4$$

$$E_a = E_a^o - (1 - \alpha) |\Delta H_r| \text{ for endothermic reaction} \quad 5$$

Kinetic parameters

By considering of the kinetic data of the present study, the parameters of rate equations presented in Table 3 were calculated and are reported in Table 4. The activation energy associated with the reaction of ethylene production from methanol (E_3) is higher than the value associated with the ethylene production reaction from DME (E_2). Therefore, ethylene mainly produced from DME at lower temperature. As temperature rises to higher values, the ethylene primarily produced from methanol. As a result, the ethylene which has just been produced at lower temperatures is more likely to be react with methanol in the hydrocarbon pool inside the Hierarchical pores. At higher

temperatures, ethylene tends to be more reactive with DME. In comparison with the kinetic data reported by [10] on conventional SAPO-34, the activation energy for production of saturated hydrocarbons has been increased in the present work, which is fully consistent with laboratory data.

Table 4. The kinetic coefficients of the MTP process.

Reaction	K_{0j}	E_j
$r_1 = k_{01} \cdot \exp\left(-\frac{E_1}{RT}\right) \cdot C_{MeOH}^2 - \frac{k_{01}}{K} \cdot \exp\left(-\frac{E_1}{RT}\right) \cdot C_{DME} \cdot C_{H_2O}$	3.2×10^5	73.2
$r_2 = k_{02} \cdot \exp\left(-\frac{E_2}{RT}\right) \cdot C_{DME}$	1.2×10^6	65.1
$r_3 = k_{03} \cdot \exp\left(-\frac{E_3}{RT}\right) \cdot C_{MeOH}$	2.6×10^6	103.2
$r_4 = k_{04} \cdot \exp\left(-\frac{E_4}{RT}\right) \cdot C_{DME} \cdot C_{C_2H_4}$	2.3×10^5	55.1
$r_5 = k_{05} \cdot \exp\left(-\frac{E_4}{RT}\right) \cdot C_{MeOH} \cdot C_{C_2H_4}$	3.4×10^5	43.9
$r_6 = k_{06} \cdot \exp\left(-\frac{E_6}{RT}\right) \cdot C_{DME} \cdot C_{C_3H_6}$	2.1×10^6	76.1
$r_7 = k_{07} \cdot \exp\left(-\frac{E_7}{RT}\right) \cdot C_{MeOH} \cdot C_{C_3H_6}$	2.6×10^6	65.7
$r_8 = k_{08} \cdot \exp\left(-\frac{E_8}{RT}\right) \cdot C_{DME} \cdot C_{C_4H_8}$	3.1×10^6	87.4
$r_9 = k_{09} \cdot \exp\left(-\frac{E_9}{RT}\right) \cdot C_{MeOH}$	1.6×10^6	125.3
$r_{10} = k_{010} \cdot \exp\left(-\frac{E_{10}}{RT}\right) \cdot C_{CO} \cdot C_{H_2O}$	2×10^6	121.1
$r_{11} = k_{11} \cdot \exp\left(-\frac{E_{11}}{RT}\right) \cdot C_{MeOH} \cdot C_{H_2}$	1.2×10^6	116.5
$r_{12} = k_{012} \cdot \exp\left(-\frac{E_{12}}{RT}\right) \cdot C_{C_2H_4} \cdot C_{H_2}$	1.6×10^6	122.1
<p>Note1 : if $j = 2,3$ $[k_{0j}] = \frac{m^3}{gr \cdot hr}$ for other $[k_{0j}] = \frac{(m^3)^2}{gr \cdot mol \cdot hr}$</p> <p>Note2 : $[E_j] = \frac{kJ}{mol}$</p>		

Results of proposed model

Fig.4 shows the amounts of ethylene and propylene calculated by the model compared with those obtained from experimental data in the fix bed reactor. Comparison of the experimental and predicted data shows that the predicted values from the proposed model are well fitted to the experimental data. As shown in these figures, almost symmetrical distribution of the data points on both sides of the parity plot's diagonal was obtained for all variables.

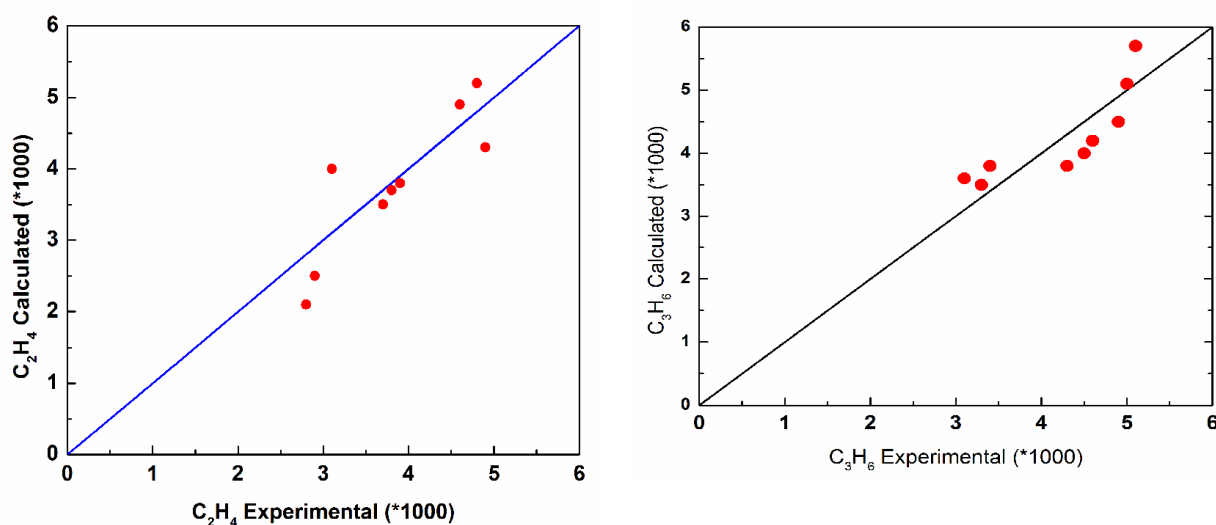


Figure 4. Experimental and calculated yields for ethylene and propylene on Ce-H-SAPO-34. T = 390–450 °C, P = 1.0 bar, t = 1–4 g cat h/mol MeOH.

Conclusions

In this study, Ce-H-SAPO-34 nanostructure catalysts were synthesized by sequential hydrothermal and impregnation methods. A new lumped kinetic model was proposed for the methanol to propylene process on Ce-H-SAPO-34 catalyst. The kinetic parameters were estimated successfully using a decimal genetic algorithm. Comparison of the experimental and predicted data showed that the predicted values from the presented model fit properly to the experimental data.

Reference

- [1]. C.N. Eng, B.V. Arnold, *Fundamental Topics in Ethylene Production, AIChE Spring National Meeting, Session, 16* (1998).
- [2]. T. Álvaro-Muñoz, E. Sastre, C. Marquez-Alvarez, *Catal. Sci. Technol.*, 4, 4330 (2014).
- [3]. Q. Sun, Y. Ma, N. Wang, X. Li, D. Xi, J. Xu, F. Deng, K.B. Yoon, P. Oleynikov, O. Terasaki, *J. Mater. Chem A.*, 42, 17828 (2014).
- [4]. C. Wang, M. Yang, P. Tian, S. Xu, Y. Yang, D. Wang, Y. Yuan, Z. Liu, *J. Mater. Chem A.*, 3, 5608 (2015).
- [5]. D.P. Serrano, J.M. Escola, P. Pizarro, *Chem. Soc. Rev.*, 42, 4004 (2013).
- [6]. Q.i. Guozhen, Z. Xie, Q. Chen, *Chem. React. Eng and Technol.*, 28 (6), 506 (2012).
- [7]. D. Lesthaeghe, S. Van, G.B. Marin, M. Waroquier, *Angew. Chem. Int. Ed.*, 45, 1714, (2006).

- [8]. D.M. Marcus, K.A. McLachlan, M.A. Wildman, J.O. Ehresmann, P.W. Kletnieks, J.F.Haw, *Angew. Chem. Int. Ed.*, 45, 3133 (2006).
- [9]. U. Olsbye, M. Bjørgen, S. Svelle, K.P. Lillerud, S.Kolboe, *Catal. Today.*, 106, 108, (2005).
- [10]. A.T.Najafabadi, S. Fatemi, M. Sohrabi, *J. Ind. Eng. Chem.*, 18 (1), 29 (2012).
- [11]. M. Ghalbi-Ahangari, P. Rashidi-Ranjbar, A. Rashidi, M. Teymuri, *React. Kin. Mech. and Catal.*, 122, 1265 (2017).
- [12]. M.M.J. Treacy, J.B. Higgins, 4th *Structure Commission of the International Zeolite Association, Amsterdam, Netherlands.*, 380, (2001).
- [13]. S.H. Jung, J.H. Lee, J.S. Chang, *Microporous Mesoporous Mater*, 112, 178 (2008).
- [14]. J. Li, Z. Li, D. Han, J. Wu, *J. Powder Technol*, 262, 177 (2014).
- [15]. A.G. Gayubo, A. T.A. guayo, A.E. Sánchez, *Ind. Eng. Chem. Res.*, 39 (2), 292 (2000).
- [16]. A.N.R. Bos, P.J.J. Tromp, H.N. Akse, *Ind. Eng. Chem. Res.*, 34(11), 3808 (1995).
- [17]. T.Y. Park, G.F. Froment, *Ind. Eng. Chem. Res.*, 40, 4172 (2001).
- [18]. T.Y. Park, G.F. Froment, *Ind. Eng. Chem. Res.*, 40, 4187, (2001).
- [19]. M. Abraha, *Chem. Eng. Dept., Texas A&M University.*, (2001).
- [20]. M. Maeder, Y.M. Neuhold, G. Puxty, *Chemom. Intell. Lab. Syst., Lab. Inf. Manage.*, 70 (2), 193 (2004).
- [21]. C.B. Lucasius, G. Kateman, *Chemom. Intell. Lab. Syst.*, 25,99 (1994).
- [22]. M. Maeder, Y. M. Neuhold, G.Puxty, P. King, *Phys. Chem. Chem. Phys.*, 5,2836 (2003).
- [23]. M.Evans, M.Polanyi, *Trans. Faraday Soc.*, 34, 11 (1938).